

Double Rydberg anions with solvated ammonium kernels: Electron binding energies and Dyson orbitals

Cite as: J. Chem. Phys. **151**, 054301 (2019); <https://doi.org/10.1063/1.5113614>

Submitted: 05 June 2019 . Accepted: 11 July 2019 . Published Online: 01 August 2019

Manuel Díaz-Tinoco , and J. V. Ortiz 



View Online



Export Citation



CrossMark

ARTICLES YOU MAY BE INTERESTED IN

[Adventures in DFT by a wavefunction theorist](#)

The Journal of Chemical Physics **151**, 160901 (2019); <https://doi.org/10.1063/1.5116338>

[Perspective: Computational chemistry software and its advancement as illustrated through three grand challenge cases for molecular science](#)

The Journal of Chemical Physics **149**, 180901 (2018); <https://doi.org/10.1063/1.5052551>

[Fantasy versus reality in fragment-based quantum chemistry](#)

The Journal of Chemical Physics **151**, 170901 (2019); <https://doi.org/10.1063/1.5126216>



Lock-in Amplifiers

Zurich Instruments

Watch the Video

Double Rydberg anions with solvated ammonium kernels: Electron binding energies and Dyson orbitals

Cite as: J. Chem. Phys. 151, 054301 (2019); doi: 10.1063/1.5113614

Submitted: 5 June 2019 • Accepted: 11 July 2019 •

Published Online: 1 August 2019



View Online



Export Citation



CrossMark

Manuel Díaz-Tinoco  and J. V. Ortiz^{a1} 

AFFILIATIONS

Department of Chemistry and Biochemistry, Auburn University, Auburn, Alabama 36849-5312, USA

^{a1}Electronic mail: ortiz@auburn.edu

ABSTRACT

Ab initio electron-propagator calculations on the electron detachment energies and associated Dyson orbitals of $N_nH_{3n+1}^-$ for $n = 1-5$ confirm the assignment of low-energy peaks in anion photoelectron spectra to double Rydberg anions, species in which a closed-shell cation binds a diffuse pair of electrons. The most stable double Rydberg anions contain $N_nH_{3n+1}^+$ cores, wherein the NH_4^+ kernel forms $n - 1$ hydrogen bonds with ammonia molecules. Other low-energy peaks for a given n pertain to double Rydberg anions of lower n that are weakly bound to ammonia molecules. High-energy peaks arise from the most stable isomers which consist of hydrides bound to N–H bonds of coordinating ammonia molecules. Dyson orbitals of electron detachment are distributed over the periphery of the bonding regions of the $N_nH_{3n+1}^+$ cores. For $n = 2-4$, negative charge accumulates mostly outside the N–H bonds of the NH_4^+ kernels that are not engaged in hydrogen bonds. For the tetrahedral cases, where $n = 1, 5$, Dyson orbitals are diffuse, symmetric functions that are orthogonalized to occupied a_1 orbitals of the cationic core. Shake-up features in spectra have been assigned to doublet states with a single diffuse electron in an s, p, d, or f orbital.

Published under license by AIP Publishing. <https://doi.org/10.1063/1.5113614>

I. INTRODUCTION

Two dots or a line may represent a pair of electrons in the elementary notations of organic and main-group inorganic chemistry. Bond and lone pairs represented thusly correspond to functions that exhibit interference between valence atomic orbitals and that are used to construct many-electron wave-functions of ground states. *Double Rydberg anions (DRAs) depart from these precedents, for in their ground states each has an electron pair that is described chiefly by diffuse orbitals.*

Persistent peaks of low electron binding energy in the photoelectron spectrum of anions with the formula NH_4^- led Bowen and co-workers to propose the existence of a double Rydberg anion in mass-selected samples alongside the more stable species, an ion-molecule complex of H^- and NH_3 .^{1,2} Evidence for the latter complex was provided by a sharp principal (X) peak that was easily assigned to electron detachment from the hydride in the stabilizing presence of the ammonia molecule's electrostatic field. A satellite peak

(A) at higher energy, whose displacement from X coincided with a symmetric-stretch excitation of ammonia, provided verification of the presence of the $H^-(NH_3)$ complex. Only careful examination of the low-energy region of the spectrum revealed the presence of a sharp peak (B) whose relative intensity varied with the conditions of anion synthesis. The ND_4^- spectrum produced the expected reduction in the separation between peaks X and A. However, the possibility of B being a hot band (i.e., one where the initial anionic state is vibrationally excited) was discounted by this peak's failure to shift position after deuteration. Electron-propagator (EP) calculations have shown that double Rydberg anions have two diffuse electrons whose largest amplitudes in Dyson orbitals for electron detachment lie chiefly outside the bonding regions of a molecular cation.³

Computational investigations³⁻¹¹ have demonstrated that the tetrahedral anion is a stable species with vibrational frequencies and electron detachment energies that coincide very closely with experimental data.³ Bond lengths change little when an electron is

removed to form the tetrahedral NH_4 radical,^{12–20} which is capable of forming covalent bonds in a manner similar to that of alkali atoms.^{21–26} The two most diffuse electrons occupy a totally symmetric orbital with two radial nodes, one of which occurs near the hydrogen nuclei. In the united atom limit of Na^- , the latter orbital correlates with $3s$, a function which also has two radial nodes. Photoelectron–photofragment coincidence spectroscopy and quantum dynamics calculations have confirmed the resemblance between the diffuse orbitals of tetrahedral NH_4^- and Na^- .²⁷

Photoelectron experiments on $\text{N}_n\text{H}_{3n+1}^-$ anions have indicated that more than one kind of diffuse species can coexist with $\text{H}^-(\text{NH}_3)_n$ complexes in a mass-selected photoelectron spectrum.^{28,29} When $n = 2$, tetrahedral NH_4^- may enter into an anion–dipole complex with NH_3 or two diffuse electrons may occupy the periphery of an N_2H_7^+ cation with a hydrogen bond between the nitrogen nuclei.^{30,31} EP calculations on electron detachment energies of all N_2H_7^- species are within the 0.02 eV error bars of experimental peaks and provide quantitative agreement with vibrational satellites seen in the low-energy region of the photoelectron spectrum. Plots of Dyson orbitals clearly show the diffuse, nonvalence character of the least bound electrons and explain the minimal effects of electron detachment on the equilibrium geometries of the uncharged, final states.

Peaks in photoelectron spectra with $n = 3, 4, 5$ were assigned to the following types of anions:^{28,29}

1. Hydrides coordinated to n ammonia molecules or $\text{H}^-(\text{NH}_3)_n$.
2. Anions with no hydrogen bridges between nitrogen atoms in which $n - 1$ ammonia molecules coordinate weakly (i.e., via charge–multipole or other relatively weak forces) to tetrahedral NH_4^- . These anions may be represented by the formula $\text{NH}_4^-(\text{NH}_3)_{n-1}$.
3. Anions form m ($1 \leq m \leq 4$, $m \leq n - 1$) hydrogen bonds between the central nitrogen atom and m nitrogen atoms in a first coordination shell and have $n - m - 1$ weakly coordinating ammonia molecules. This type is represented as $\text{N}_{m+1}\text{H}_{3m+4}^-(\text{NH}_3)_{n-m-1}$.

In all of these spectra, the most intense peak belongs to the most abundant species, the hydride–ammonia complex, $\text{H}^-(\text{NH}_3)_n$. However, the relative intensity of certain low-energy peaks can rise markedly for several values of n . For example, when $n = 5$, the single, low-energy peak has an intensity that is approximately one fifteenth that of the hydride–ammonia complex. This result suggests that completion of the first coordination shell of four hydrogen bonds around a central tetrahedral unit endows the anion with greater stability. The authors of these experiments have suggested that completion of a second solvation sphere and concomitant enhanced abundance may occur for the cluster with $n = 17$.

The fate of diffuse electrons with increasing n remains uncertain, especially in cases where $m = n - 1$. They could be expelled to the periphery of the cluster near the external hydrogens, distributed over the interstices between N–H and N–H–N bonding regions or assigned to antibonding orbitals that are stabilized by delocalization. EP calculations that produce convincing assignments of the photoelectron spectra will also yield Dyson orbitals whose amplitudes can solve these puzzles.

In a simple one-electron picture of photodetachment where an initial state is defined by a single configuration, a 2hp correlation

final state corresponds to a configuration where two occupied (h) spin–orbitals of the initial state are vacant and a virtual (p) spin–orbital is occupied. Pole strengths for electron detachment to such states vanish, i.e., the transition is forbidden with a one-electron transition operator such as the dipole moment. After inclusion of electron interaction in the initial state, the resulting configuration mixing leads to nonvanishing pole strengths for correlation final states. The appearance of such states is evident for the importance of correlation in the initial state. (Configuration mixing in the final states also affects the values of the pole strengths.) Because ground state correlation in double Rydberg and related anions is strong, one may expect to find 2hp correlation states that lie at spectroscopically accessible energies above those of the ground-state doublet radicals.

Photoelectron spectra of $\text{N}_n\text{H}_{3n+1}^-$ for $n = 4–6$ exhibit such higher-energy transitions.²⁹ Fuke and co-workers observed excited states in the spectra of $\text{N}_n\text{H}_{3n+1}$ clusters and assigned them to NH_4 Rydberg (np to ns) emissions perturbed by the presence of ammonia molecules.^{32,33} There is a close resemblance between peak separations in the anion photoelectron spectra and the transition energies reported for the uncharged species.²⁹ Correlation final states from the photoionization of double Rydberg anions may have a single electron in a diffuse orbital with different spatial and nodal characteristics from those that characterize the Dyson orbital for the lowest detachment energy.

To interpret these spectral features, electron affinities of cations at the geometries of the anions will be calculated. Excitation energies of uncharged radicals and therefore electron detachment energies that lead to correlation states may be inferred from differences between electron affinities.

II. METHODS

Structures of anions were optimized at the coupled-cluster singles and doubles (CCSD) level³⁴ with the 6-311++G(d,p) basis set^{35–37} plus extra diffuse functions (exponents: H s 0.010 80 and N sp 0.019 17). All frequencies were real except for tetrahedral N_5H_{16} , which has small imaginary frequencies due to the excess of diffuse functions; optimization without extra diffuse functions yields real frequencies and negligible change in the structure. Brueckner–doubles coupled-cluster (BD)^{38,39} calculations were performed with the valence-only orbital optimization and no-symmetry options. Two-electron integral accuracy was set to 10^{-20} a.u. and self-consistent field accuracy was set to 10^{-10} a.u. because of the abundance of diffuse functions.⁴⁰ Brueckner–doubles, triple-operator-manifold (BDT1) electron propagator calculations^{41–44} were performed with the 6-311++G(2df,2pd) basis set plus the same extra diffuse functions used for geometry optimizations. All pole strengths (norms of Dyson orbitals) were 0.85 or higher.

All calculations were executed with the development version of Gaussian.⁴⁵

Dyson orbitals of electron detachment from anions with N electrons, defined by

$$\phi^{\text{Dyson}}(x_1) = N^{0.5} \int \Psi_{\text{anion}}(x_1, x_2, x_3, \dots, x_N) \times \Psi_{\text{neutral}}^*(x_2, x_3, x_4, \dots, x_N) dx_2 dx_3 dx_4 \dots dx_N,$$

and of electron attachment to cations with $N - 2$ electrons, defined by

$$\phi^{\text{Dyson}}(x_1) = (N - 1)^{0.5} \int \Psi_{\text{neutral}}(x_1, x_2, x_3, \dots, x_{N-1}) \times \Psi_{\text{cation}}^*(x_2, x_3, x_4, \dots, x_{N-1}) dx_2 dx_3 dx_4 \dots dx_{N-1},$$

were plotted using Gaussview⁴⁶ from a cube file generated with an enhanced edge size in Molden.⁴⁷ Isovalues in the orbital plots equal 0.02 for $n = 1-3$ or 0.012 for $n = 4, 5$.

III. RESULTS AND DISCUSSION

Tables I–III and Figures 1–7 display numerical and graphical results on various isomers of $N_n H_{3n+1}^-$.

For $n = 1$, the hydride–ammonia complex is considerably more stable than the tetrahedral double Rydberg anion (DRA), which is henceforth denoted as NH_4^- . In the former anion, the free hydride's vertical electron detachment energy (VEDE) of 0.75 eV is increased by the electrostatic potential of the coordinated ammonia molecule. A single N–H bond in NH_3 approaches the hydride in a C_s structure and increases the VEDE by more than 0.3 eV. The Dyson orbital is dominated by diffuse hydride s functions, which are in an antibonding relationship with valence functions on the closest N–H bond (see Fig. 1). In the DRA, a totally symmetric Dyson orbital for the lowest VEDE has its largest amplitudes beyond the H nuclei. Two radial nodes anticipate the 3s united-atom limit for this orbital. Bond

TABLE II. $N_n H_{3n+1}^+$ electron affinities and $N_n H_{3n+1}$ excitation energies (eV).

n	EA ₀	EA ₁	EA ₂	EES-theory	EE-expt. ²⁹	EE-expt. ^{32,33}
4	2.814	2.111	2.069	0.70, 0.75	0.83	0.81
5	2.570	1.988		0.58	0.70	0.71

lengths are nearly unchanged in the DRA with respect to the tetrahedral radical or cation and therefore confirm the unimportance of antibonding character in the Dyson orbital. The VEDE is close to 0.5 eV and resembles those of alkali-metal anions (e.g., 0.55 eV for Na^-). Energetic instability of the DRA with respect to the hydride–ammonia complex accounts for the low relative intensity of the peak observed at 0.47 eV, a datum that is in very close agreement with the present theory.

Three structures pertain to the photoelectron spectrum where $n = 2$.²⁸ The most stable is a complex of a hydride anion with two coordinated ammonia molecules in a C_2 arrangement. Addition of a second ammonia molecule to $H^-(NH_3)$ results in a VEDE that has increased by approximately 0.4 eV. The Dyson orbital remains localized on the hydride's nucleus with slight delocalization onto the ammonia molecules. It is also possible to add an ammonia molecule to the NH_4^- DRA. In the resulting $NH_4^-(NH_3)$ complex, the VEDE is approximately 0.1 eV larger than its counterpart in NH_4^- , for the coordinating ammonia molecule orients its protons toward the tetrahedral anion. Minor delocalization occurs in the Dyson orbital,

TABLE I. $N_n H_{3n+1}^-$ isomerization and electron binding energies (eV).

n	Isomer	$\Delta E_{\text{isomer}}^{BD}$	Theory	Expt. ²⁸
1	$H^-(NH_3)$	0	1.079	1.110
	NH_4^-	0.49	0.477	0.472
2	$H^-(NH_3)_2$	0	1.497	1.460
	$NH_4^-(NH_3)$	0.76	0.596	0.578
	$N_2 H_7^-$	0.63	0.407	0.415
3	$H^-(NH_3)_3$	0	1.829	1.820
	$(NH_3)NH_4^-(NH_3)$	1.05	0.713	
	$NH_4^- [NH_3]_2$	0.96	0.679	0.660
	$N_2 H_7^-(NH_3)$	0.93	0.498	0.495
	$N_3 H_{10}^-$	0.73	0.398	0.424
4	$H^-(NH_3)_4$	0	2.159	2.111
	$(NH_3)_3 NH_4^-$	1.08	0.743	
	$[NH_3]_2 NH_4^-(NH_3)$	1.19	0.795	
	$NH_4^- [NH_3]_3$	1.27	0.919	
	$(NH_3)N_2 H_7^-(NH_3)$	1.16	0.860	
	$N_2 H_7^- [NH_3]_2$	1.07	0.564	
	$N_3 H_{10}^-(NH_3)$	0.97	0.471	
	$N_4 H_{13}^-$	0.72	0.398	0.427
5	$H^-(NH_3)_5$	0	2.420	2.360
	$N_5 H_{16}^-$	0.71	0.389	0.434

TABLE III. $N_n H_{3n+1}$ excitation energies (eV).

l	n	Term	Energy	n	Term	Energy
s	4	2A_1	0	5	2A_1	0
p		2E	0.703		2T_2	0.582
		2A_1	0.745			
d		2A_1	1.368		2T_2	1.200
		2E	1.390		2E	1.250
		2E	1.464			
s		2A_1	1.596		2A_1	1.409
	f		2E	1.865		2T_1
		2A_1	1.921		2T_2	1.757
		2A_2	1.956		2A_1	1.913
		2E	2.143			
		2A_1	2.156			
p		2E	2.370		2T_2	2.177
		2A_1	2.373			
d		2E	2.424		2T_2	2.193
		2A_1	2.547		2E	2.200
		2E	2.572			

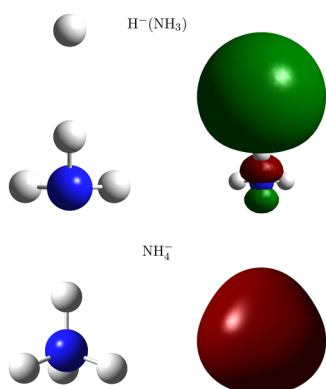


FIG. 1. $n = 1$ structures and Dyson orbitals of electron detachment from anions.

which is dominated by diffuse functions on the periphery of the tetrahedral anion. In the remaining isomer, the cationic core that binds two diffuse electrons has a hydrogen bond between the N nuclei. A VEDE that is smaller than that of DRA NH_4^- corresponds to a Dyson orbital whose largest diffuse amplitudes are enclosed by a green, concave contour that lies chiefly outside the nonbridging H nuclei of the tetrahedral NH_4^- kernel of the N_2H_7^- DRA. Orthogonalization to valence s functions on the N atoms results in the red contours. Plots of lower isovalues disclose significant delocalization to regions beyond the H nuclei of the NH_3 fragment of this DRA. Amplitudes near the hydrogen bridge are negligible in this isomer. This structure is slightly more stable than the $\text{NH}_4^-(\text{NH}_3)$ complex. For all three VEDEs, agreement between theory (present and past³¹) and experiment is excellent.

Coordination of an ammonia molecule with weak interactions to the three latter structures accounts for all isomers with $n = 3$ except one. A third coordinating ammonia molecule increases the VEDE of $\text{H}^-(\text{NH}_3)_3$ by about 0.35 eV over that of $\text{H}^-(\text{NH}_3)_2$. In the latter structure, the Dyson orbital remains localized on the hydride. Antibonding relationships with three equivalent N–H bond functions can be seen. Weak interactions between ammonia molecules account for the pyramidal, C_3 structure. Two structures can be anticipated for the coordination of an ammonia molecule to $\text{NH}_4^-(\text{NH}_3)$: it could approach the DRA fragment with its protons to form $(\text{NH}_3)\text{NH}_4^-(\text{NH}_3)$ or participate in a hydrogen bond with the already present NH_3 to form $\text{NH}_4^+[\text{NH}_3]_2$. The latter option is energetically favored by 0.11 eV and results in a DRA that is stabilized by the electrostatic potential of $[\text{NH}_3]_2$. (Square brackets designate a hydrogen-bonded cluster.) An increase of 0.08 eV with respect to $\text{NH}_4^-(\text{NH}_3)$ occurs for the VEDE of $\text{NH}_4^+[\text{NH}_3]_2$. Localization of the Dyson orbital on the tetrahedral DRA fragment is conserved; only a small red contour is seen on the neighboring ammonia molecule. No distinct peak in the photoelectron spectrum corresponds to the less stable $(\text{NH}_3)\text{NH}_4^-(\text{NH}_3)$ structure, although the predicted VEDE is only 0.03 eV larger than that of $\text{NH}_4^+[\text{NH}_3]_2$. (Because such a feature would correspond to a less stable structure, it is possible that it is obscured by the broad vibrational satellite that lies at 0.824 eV in the spectrum.²⁸) In the $\text{N}_2\text{H}_7^-(\text{NH}_3)$ complex, the N_2H_7^- DRA is approached by an ammonia molecule whose protons

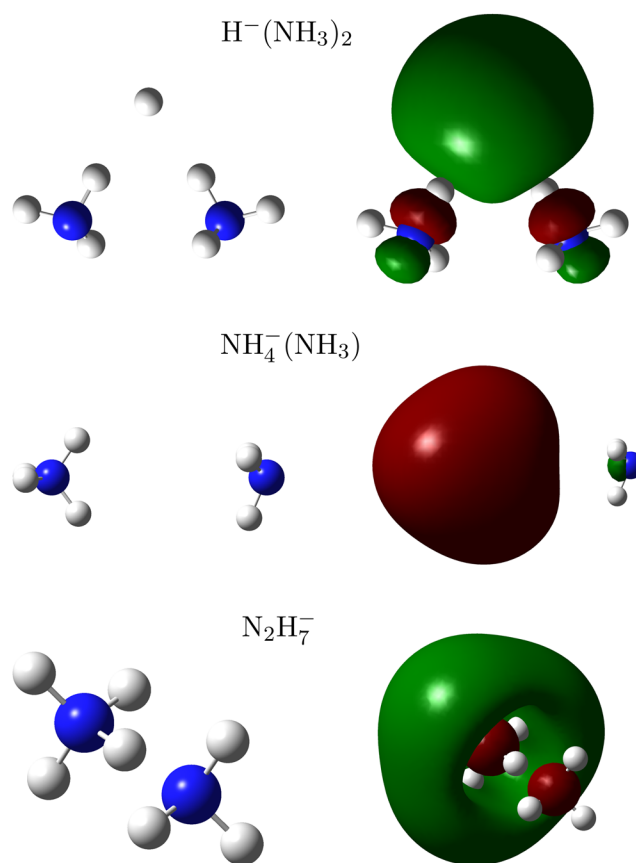
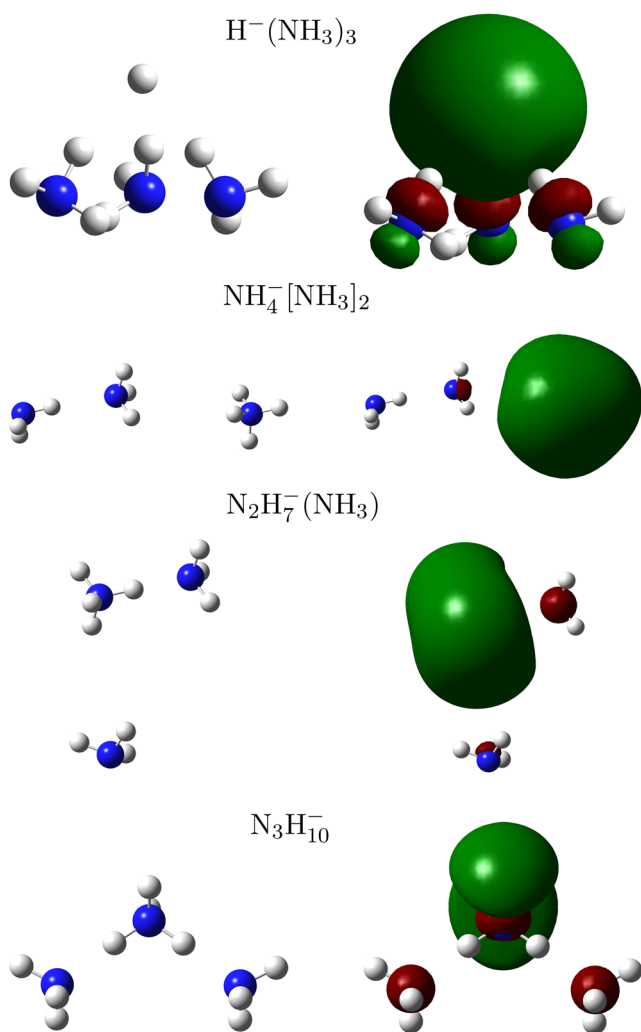


FIG. 2. $n = 2$ structures and Dyson orbitals of electron detachment from anions.

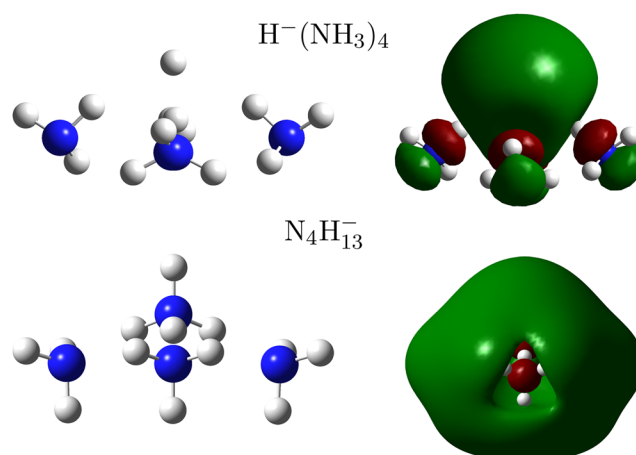
are oriented toward the DRA's diffuse electrons. An initial geometry with an approximately linear arrangement of N atoms rearranges itself during optimization to the present, bent minimum. A distortion of the diffuse Dyson orbital of DRA N_2H_7^- toward the weakly bound ammonia molecule can be seen. According to theory, the VEDE has increased by 0.9 eV from N_2H_7^- to $\text{N}_2\text{H}_7^-(\text{NH}_3)$. The last isomer displays two N–H–N hydrogen bonds and a VEDE that is within 0.01 eV of that of N_2H_7^- . Diffuse Dyson orbital amplitudes are largest outside the two nonbridging H nuclei of the tetrahedral fragment. Red contours emerge again through orthogonalization to valence N s functions in this N_3H_{10} DRA, which is the most stable isomer except for the $\text{H}^-(\text{NH}_3)_3$ complex. In all cases, the assignments of VEDEs to anionic structures made on the basis of spectra are confirmed.²⁸

Whereas photoelectron spectra so far display n low-energy peaks, with each corresponding to a species with a DRA, the spectrum for $n = 4$ is considerably simpler.²⁸ The lone, low-energy peak may be assigned to a species with three N–H–N bridges between a central, tetrahedral fragment, and three neighboring ammonia molecules. This peak's intensity relative to that of the high-energy peak is markedly greater than in the previous cases.²⁸ A symmetric Dyson orbital with positive contours in green that are spread over regions outside the nonbridging H of the tetrahedral fragment

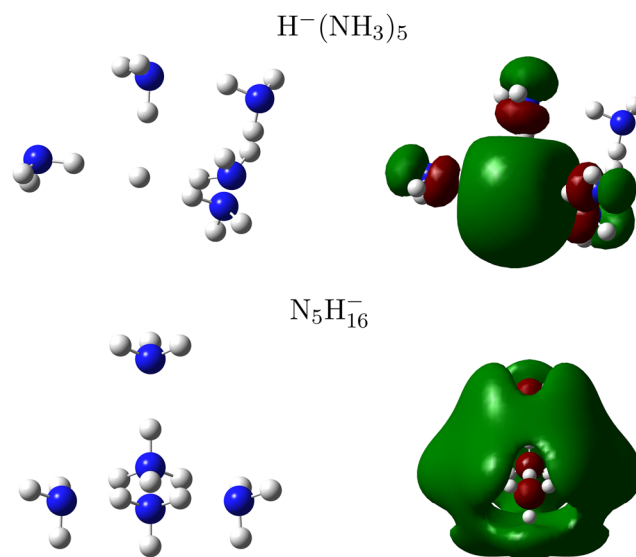
FIG. 3. $n = 3$ structures and Dyson orbitals of electron detachment from anions.

and the nine H nuclei of the three coordinating ammonia molecules surrounds N valence s functions of the opposite phase in red. With respect to the NH_4^- , $N_2H_7^-$, and $N_3H_{10}^-$ DRAs, an almost unchanged VEDE is predicted by theory and confirmed by experiment for the $N_4H_{13}^-$ DRA. As in the previous cases, the most intense peak still belongs to a hydride–ammonia complex with n ammonia molecules. An increment of about 0.3 eV vs $H^-(NH_3)_3$ occurs in the VEDE of $H^-(NH_3)_4$. Both predicted VEDEs are within 0.05 eV of experiment.²⁸ This complex has a C_2 axis and four ammonia molecules below a perpendicular plane that includes the hydride's nucleus. Diffuse s functions on the hydride are the most important contributors to the Dyson orbital; antibonding relationships with N–H bond functions are present.

Other isomers that contain NH_4^- , $N_2H_7^-$, or $N_3H_{10}^-$ DRAs with weakly coordinated ammonia molecules are less stable and have VEDEs that are predicted to be higher than that of the $N_4H_{13}^-$ DRA. In these still unobserved structures, stability grows with the

FIG. 4. $n = 4$ structures and Dyson orbitals of electron detachment from anions.

formation of hydrogen bonds in larger $N_nH_{3n+1}^-$ DRAs and the reduction of weak interactions that involve ammonia molecules or clusters. The cluster denoted $(NH_3)_3NH_4^-$ has C_{3v} symmetry and three ammonia molecules with H nuclei oriented toward the tetrahedral NH_4^- DRA. Greater stability of 0.1 eV in the $[NH_3]_2NH_4^-(NH_3)$ cluster follows from the formation of a hydrogen-bonded ammonia dimer. This trend continues in the $NH_4^-[NH_3]_3$ case, where an ammonia trimer binds to the NH_4^- DRA with an additional stabilization of 0.12 eV. A similar reduction in energy, 0.11 eV, occurs between the $(NH_3)N_2H_7^-(NH_3)$ and $N_2H_7^-[NH_3]_2$ clusters. Observation of the $NH_4^-[NH_3]_2$ and $N_2H_7^-(NH_3)$ clusters in the photoelectron spectrum where $n = 3$ and their low relative energies of 0.7 eV suggest that the $N_3H_{10}^-(NH_3)$ cluster may also be synthesized and interrogated spectroscopically.

FIG. 5. $n = 5$ structures and Dyson orbitals of electron detachment from anions.

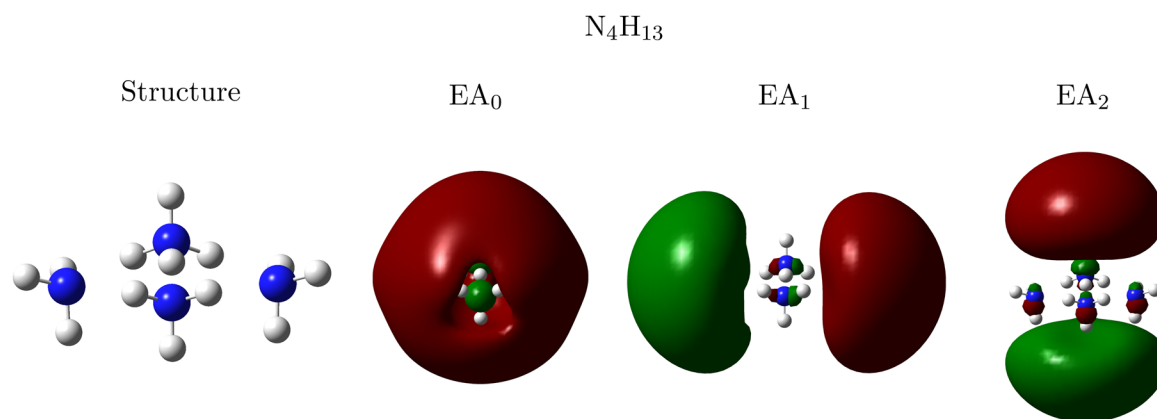


FIG. 6. $N_4H_{13}^-$ structure and Dyson orbitals of electron attachment to cation.

For $n = 5$, the photoelectron spectrum again displays only two important peaks and the relative intensity of the low VEDE peak is enhanced even further.²⁸ The first belongs to a hydride-ammonia complex in which the VEDE rises again with coordination number; the increment this time is only 0.25 eV. Diffuse s functions on the hydride nucleus continue to dominate the Dyson orbital. Instead of adding to the primary solvation shell of the anion, the fifth ammonia molecule forms hydrogen bonds with two ammonia molecules that are coordinated to the hydride. The $N_5H_{16}^-$ DRA now has a completed solvation sphere for the central tetrahedral fragment, for there are four H-N-H bridges with surrounding ammonia molecules. A practically unchanged VEDE with respect to the DRAs for $n = 2, 3, 4$ is predicted by theory and confirmed convincingly by experiment. A symmetric Dyson orbital whose amplitudes in green reside chiefly outside the 12 peripheral H nuclei displays nodes that result in red s -like contours on the N centers.

There is no clear relationship between the relative intensities of $H^-(NH_3)_3$ and DRA peaks and the corresponding isomerization

energies. The higher relative intensities of DRA peaks for $n = 4, 5$ pertain to isomerization energies in excess of 0.7 eV, but the relatively faint DRA peak for $n = 1$ is accompanied by an isomerization energy of only 0.5 eV. These results suggest that the experimental samples are far from equilibrium.

Additional peaks in anion photoelectron spectra for $n = 4, 5$ may be assigned to correlation final states that have a single electron in an orbital that does not resemble the Dyson orbitals depicted so far. Such states are easily accessed computationally by calculating, at anionic geometries, electron affinities of closed-shell cations. Differences between electron affinities constitute excitation energies (EEs) of uncharged radicals, which may also be inferred from differences of electron detachment energies in photoelectron spectra²⁹ (see Table II). The largest electron affinity for a cation at the geometry of a DRA is denoted as EA_0 , for it corresponds to the doublet radical's ground state, labeled 2A_1 for both values of n . Dyson orbitals for these electron affinities resemble their counterparts for the electron detachment energies of the anions. Smaller electron affinities

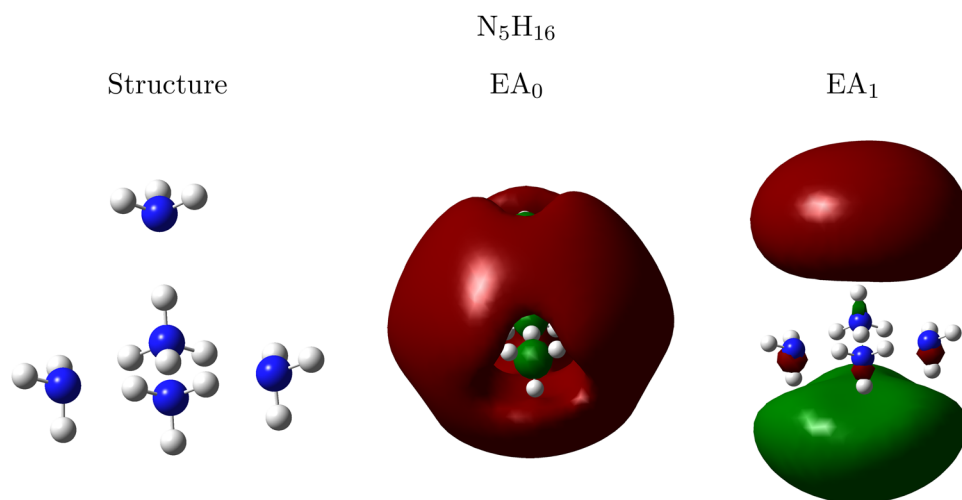


FIG. 7. $N_5H_{16}^-$ structure and Dyson orbitals of electron attachment to cation.

imply radical excitation energies that may be compared with values inferred from spectra. Predicted excitation energies are in excellent agreement with anion photoelectron spectra²⁸ and excitation spectra of the corresponding radicals.^{32,33} (Close agreement between the two experimental techniques indicates only minor nuclear relaxation between uncharged and anionic clusters.) Energetic data in Tables I and II strongly suggest that correlation final states for electron detachment from the $N_4H_{13}^-$ and $N_5H_{16}^-$ DRAs are responsible for the peaks seen at 1.26 and 1.13 eV, respectively, in anion photoelectron spectra.²⁹ Dyson orbitals for the largest electron affinities of cations with $n = 4, 5$ display nodes that resemble those of Dyson orbitals of electron detachment from anions (see Figs. 6 and 7). For the second electron affinity of the cation (EA_1) where $n = 5$, the Dyson orbitals resemble diffuse p orbitals that have been orthogonalized to N–H bonding functions. The 2T_2 state of N_5H_{16} is threefold degenerate. Its counterparts for $n = 4$, where the C_{3v} point group obtains, exhibit a small energy difference (EA_1 vs EA_2) of 0.05 eV between the higher p_z level and the degenerate p_x and p_y cases. (Only one member of the latter degenerate pair is shown in Fig. 6.) Energies of higher excited states of N_4H_{13} and N_5H_{16} at the geometries of their respective anions are displayed in Table III. Excitation energies are larger for $n = 4$ than for $n = 5$. Approximate l quantum numbers that are based on a hydrogenic characterization of the Dyson orbitals may be inferred from the angular nodes for the corresponding cationic electron affinities. For the two radicals, a common pattern can be discerned: s, p, d, s, f, p, and d. These states correspond to anion electron detachment energies of approximately 3 eV or less and therefore may be observed with current experimental techniques.

IV. CONCLUSIONS

The most stable double Rydberg anion with the formula $N_nH_{3n+1}^-$ for $n = 1-5$ has a tetrahedral NH_4^+ kernel with hydrogen bonds to $n - 1$ NH_3 proton acceptors and a diffuse pair of electrons that occupies space beyond the exterior N–H bonds. Less stable species of the same formula consist of double Rydberg anions of the most stable kind with lower n that are coordinated to ammonia molecules through attractions between the negative ion and positively charged regions of ammonia molecules or clusters. For $n = 1-4$, global energy minima have hydride anions coordinated to n NH_3 molecules through approximately linear $H^- - HN$ linkages. For $n = 5$, the global minimum is a tetracoordinate hydride joined by an ammonia molecule that forms hydrogen bonds with two other molecules instead of interacting directly with the anionic center.

Assignments of peaks in anion photoelectron spectra to electron detachment energies of such species²⁸ have been confirmed by electron propagator calculations that are in close numerical agreement. The most stable double Rydberg anions for a given n have vertical electron detachment energies of about 0.4 eV for $n = 2-5$; the result for $n = 1$ is slightly higher at 0.47 eV. Other low-energy peaks pertaining to complexes of double Rydberg anions with ammonia molecules have higher vertical electron detachment energies of 0.5–0.7 eV. The high-energy peaks above 1 eV belong to hydride–ammonia complexes.

Dyson orbitals of electron detachment of the most stable double Rydberg anions are distributed over the periphery of hydrogen-bonded $N_nH_{3n+1}^-$ cores. For cases where the T_d point group is

relevant, i.e., $n = 1, 5$, the Dyson orbital resembles a diffuse s function that has been orthogonalized to occupied a_1 orbitals. For $n = 2-4$, regions outside the hydrogens of the NH_4^+ kernels that are not engaged in hydrogen bonds accumulate the most electronic charge and phases in the Dyson orbitals change in the interior of the cationic cores. Coordination to an ammonia molecule or cluster introduces only slight distortions to Dyson orbitals of the most stable double Rydberg anions. In the hydride–ammonia complexes, Dyson orbitals consist chiefly of diffuse s functions centered on the hydride nucleus; minor delocalization and antibonding relationships are visible on coordinated N–H bonds.

At the geometries of the most stable double Rydberg anions, Dyson orbitals for the largest electron attachment energy to the cationic core strongly resemble those of electron detachment of the anion. For both electron binding energies, the final state is the same uncharged doublet. By calculating smaller electron attachment energies of the cation, it is possible to access the excited states of the doublet radicals. Dyson orbitals with diffuse s, p, d, and f nodal patterns emerge for these states. In anion photoelectron spectra for $n = 4-6$, higher electron detachment energies have been assigned to excited neutral states of this kind.²⁹ Excitation energies of the radicals inferred from the present calculations and from spectra are in close agreement and confirm the Rydberg characterization of the excited states. In qualitative terms, these states are reached from the anion through simultaneous removal of an electron from the Dyson orbital of the lowest electron detachment energy and excitation from the same orbital to a more diffuse function, i.e., through a shake-up process. The presence of these spectral features underlines the importance of electron correlation in the ground-state of the anion, for their intensities are within an order of magnitude of those that pertain to the ground states of the radicals.

ACKNOWLEDGMENTS

The authors thank Professor Filip Pawłowski for technical assistance and useful conversations. This research was supported by the National Science Foundation through Grant No. CHE-1565760 to Auburn University.

REFERENCES

- 1 J. V. Coe, J. T. Snodgrass, C. B. Freidhoff, K. M. McHugh, and K. H. Bowen, “Negative ion photoelectron spectroscopy of the hydride–ammonia negative cluster ion $H^-(NH_3)_1$,” *J. Chem. Phys.* **83**(6), 3169–3170 (1985).
- 2 J. T. Snodgrass, J. V. Coe, C. B. Freidhoff, K. M. McHugh, and K. H. Bowen, “Photodetachment spectroscopy of cluster anions. Photoelectron spectroscopy of $H^-(NH_3)_1$, $H^-(NH_3)_2$ and the tetrahedral isomer of NH_4^- ,” *Faraday Discuss. Chem. Soc.* **86**, 241–256 (1988).
- 3 J. V. Ortiz, “Vertical and adiabatic ionization energies of NH_4^- isomers via electron propagator theory and many body perturbation theory calculations with large basis sets,” *J. Chem. Phys.* **87**(6), 3557–3562 (1987).
- 4 H. Cardy, C. Larrieu, and A. Dargelos, “An *ab initio* study of the tetrahedral tetrahydronitrate(1-) (NH_4^-) ion,” *Chem. Phys. Lett.* **131**(6), 507–512 (1986).
- 5 D. Cremer and E. Kraka, “Theoretical determination of molecular structure and conformation. 17. On the existence of FH_2^- , OH_3^- , NH_4^- , and CH_5^- in the gas phase,” *J. Phys. Chem.* **90**(1), 33–40 (1986).
- 6 M. Gutowski, J. Simons, R. Hernandez, and H. L. Taylor, “Double-Rydberg molecular anions,” *J. Phys. Chem.* **92**(22), 6179–6182 (1988).

- ⁷J. V. Ortiz, "Structures and properties of double-Rydberg anions," *J. Phys. Chem.* **94**(12), 4762–4763 (1990).
- ⁸J. Simons and M. Gutowski, "Double-Rydberg molecular anions," *Chem. Rev.* **91**, 669–677 (1991).
- ⁹N. Matsunaga and M. S. Gordon, "A theoretical study of NH_4^- and PH_4^- ," *J. Phys. Chem.* **99**(34), 12773–12780 (1995).
- ¹⁰J. Melin, G. Seabra, and J. V. Ortiz, "Electronic structure and reactivity in double Rydberg anions: Characterization of a novel kind of electron pair," in *Theoretical Aspects of Chemical Reactivity*, Volume 19 of Theoretical and Computational Chemistry, edited by A. Toro-Labbé (Elsevier, Amsterdam, 2007), Chap. 6, pp. 87–100.
- ¹¹J. Melin and J. V. Ortiz, " OH_3^- and O_2H_2^- double Rydberg anions: Predictions and comparisons with NH_4^- and N_2H_7^- ," *J. Chem. Phys.* **127**, 014307 (2007).
- ¹²G. Herzberg, "Rydberg spectra of triatomic hydrogen and of the ammonium radical," *Faraday Discuss. Chem. Soc.* **71**, 165–173 (1981), 4 plates.
- ¹³G. Herzberg and J. T. Hougen, "Spectra of the ammonium radical: The Schuster band of ND_4 ," *J. Mol. Spectrosc.* **97**(2), 430–440 (1983).
- ¹⁴G. Herzberg, "Spectra of the ammonium radical: The Schüler bands," *J. Astrophys. Astron.* **5**(2), 131–138 (1984), 3 plates.
- ¹⁵G. Herzberg, "Spectra of triatomic hydrogen and of the ammonium radical," *J. Mol. Struct.* **113**, 1–9 (1984).
- ¹⁶G. I. Gellene, D. A. Cleary, and R. F. Porter, "Stability of the ammonium and methylammonium radicals from neutralized ion-beam spectroscopy," *J. Chem. Phys.* **77**(7), 3471–3477 (1982).
- ¹⁷W. Ketterle, P. Grasshoff, H. Figger, and H. Walther, "Observation of the nitrogen deuteride (ND_4) Schuler band in a neutralized ion beam experiment," *Z. Phys. D: At., Mol. Clusters* **9**(4), 325–329 (1988).
- ¹⁸J. D. Savee, J. E. Mann, and R. E. Continetti, "Stability of the ground and low-lying vibrational states of the ammonium radical," *J. Phys. Chem. Lett.* **4**(21), 3683–3686 (2013).
- ¹⁹J. V. Ortiz, I. Martín, A. M. Velasco, and C. Lavín, "Ground and excited states of NH_4 : Electron propagator and quantum defect analysis," *J. Chem. Phys.* **120**(17), 7949–7954 (2004).
- ²⁰A. M. Velasco, C. Lavín, I. Martín, J. Melin, and J. V. Ortiz, "Partial photoionization cross sections of NH_4 and H_3O Rydberg radicals," *J. Chem. Phys.* **131**(2), 024104 (2009).
- ²¹A. I. Boldyrev and J. Simons, "On the possibility of mixed Rydberg-valence bonds," *J. Phys. Chem. A* **103**(18), 3575–3580 (1999).
- ²²A. I. Boldyrev and J. Simons, "Rydberg bonding in ammonium dimer ($(\text{NH}_4)_2$). [Erratum to document cited in CA117(22):220446z]," *J. Phys. Chem.* **97**(7), 1470 (1993).
- ²³A. I. Boldyrev and J. Simons, "Rydberg bonding in ammonium dimer ($(\text{NH}_4)_2$)," *J. Phys. Chem.* **96**(22), 8840–8843 (1992).
- ²⁴J. S. Wright and D. McKay, "Stability of the Rydberg dimer (NH_4)," *J. Phys. Chem.* **100**(18), 7392–7397 (1996).
- ²⁵R. Barrios, P. Skurski, and J. Simons, "Characterization of the Rydberg bonding in $(\text{NH}_4)_2$," *J. Phys. Chem. A* **104**(46), 10855–10858 (2000).
- ²⁶A. E. Ketvirtis and J. Simons, "Valence-Rydberg bonding in bimolecular $\text{R-Ca}^+\text{NH}_2\text{-R}'$ complexes," *J. Am. Chem. Soc.* **122**(2), 369–377 (2000).
- ²⁷Q. Hu, H. Song, C. J. Johnson, J. Li, H. Guo, and R. E. Continetti, "Imaging a multidimensional multichannel potential energy surface: Photodetachment of $\text{H}^-(\text{NH}_3)$ and NH_4^- ," *J. Chem. Phys.* **144**(24), 244311 (2016).
- ²⁸S.-J. Xu, J. M. Nilles, J. H. Hendricks, S. A. Lyapustina, and K. H. Bowen, "Double Rydberg anions: Photoelectron spectroscopy of NH_4^- , N_2H_7^- , $\text{N}_3\text{H}_{10}^-$, $\text{N}_4\text{H}_{13}^-$, and $\text{N}_5\text{H}_{16}^-$," *J. Chem. Phys.* **117**(12), 5742–5747 (2002).
- ²⁹D. Radisic, S. T. Stokes, and K. H. Bowen, "Two new double Rydberg anions plus access to excited states of neutral Rydberg radicals via anion photoelectron spectroscopy," *J. Chem. Phys.* **123**(1), 011101 (2005).
- ³⁰H. Hopper, M. Lococo, O. Dolgounitcheva, V. G. Zakrzewski, and J. V. Ortiz, "Double-Rydberg anions: Predictions on NH_3AH_n^- and OH_2AH_n^- structures," *J. Am. Chem. Soc.* **122**(51), 12813–12818 (2000).
- ³¹J. V. Ortiz, "A double Rydberg anion with a hydrogen bond and a solvated double Rydberg anion: Interpretation of the photoelectron spectrum of N_2H_7^- ," *J. Chem. Phys.* **117**(12), 5748–5756 (2002).
- ³²S. Nonose, T. Taguchi, K. Mizuma, and K. Fuke, "Electronic spectra of solvated NH_4 radicals $\text{NH}_4(\text{NH}_3)_n$ for $n = 1-6$," *Eur. Phys. J. D* **9**(1-4), 309–311 (1999).
- ³³S. Nonose, T. Taguchi, F. Chen, S. Iwata, and K. Fuke, "Electronic spectra and structures of solvated NH_4 radicals, $\text{NH}_4(\text{NH}_3)_n$ ($n = 1-8$)," *J. Phys. Chem. A* **106**(21), 5242–5248 (2002).
- ³⁴G. D. Purvis and R. J. Bartlett, "A full coupled-cluster singles and doubles model: The inclusion of disconnected triples," *J. Chem. Phys.* **76**, 1910–1918 (1982).
- ³⁵K. Raghavachari, J. S. Binkley, R. Seeger, and J. A. Pople, "Self-consistent molecular orbital methods. XX. Basis set for correlated wave-functions," *J. Chem. Phys.* **72**, 650–654 (1980).
- ³⁶T. Clark, J. Chandrasekhar, G. W. Spitznagel, and P. von Ragué Schleyer, "Efficient diffuse function-augmented basis sets for anion calculations. III. The 3-21+G basis set for first-row elements, Li-F," *J. Comp. Chem.* **4**, 294–301 (1983).
- ³⁷M. J. Frisch, J. A. Pople, and J. S. Binkley, "Self-consistent molecular orbital methods. 25. Supplementary functions for Gaussian basis sets," *J. Chem. Phys.* **80**, 3265–3269 (1984).
- ³⁸R. A. Chiles and C. E. Dykstra, "An electron pair operator approach to coupled cluster wave functions. Application to diatomic hydrogen, diatomic beryllium, and diatomic magnesium and comparison with CEPA methods," *J. Chem. Phys.* **74**(8), 4544–4556 (1981).
- ³⁹N. C. Handy, J. A. Pople, M. Head-Gordon, R. Krishnan, and G. W. Trucks, "Size-consistent Brueckner theory limited to double substitutions," *Chem. Phys. Lett.* **164**(2-3), 185–192 (1989).
- ⁴⁰M. Czaplá, J. Simons, and P. Skurski, "Dissociative electron attachment to HGaF_4 Lewis-Brønsted superacid," *Phys. Chem. Chem. Phys.* **20**, 21739–21745 (2018).
- ⁴¹J. V. Ortiz, "Electron detachment energies of closed-shell anions calculated with a renormalized electron propagator," *Chem. Phys. Lett.* **296**(5), 494–498 (1998).
- ⁴²J. V. Ortiz, "Single-reference electron propagator calculations on vertical ionization energies of ozone," *Chem. Phys. Lett.* **297**(3), 193–199 (1998).
- ⁴³J. V. Ortiz, "Electron propagator theory: An approach to prediction and interpretation in quantum chemistry," *Wiley Interdiscip. Rev.: Comput. Mol. Sci.* **3**(2), 123–142 (2013).
- ⁴⁴J. V. Ortiz, "Interpreting bonding and spectra with correlated, one-electron concepts from electron propagator theory," in *Annual Reports in Computational Chemistry*, edited by D. A. Dixon (Elsevier, 2017), Vol. 13, Chap. 4, pp. 139–182.
- ⁴⁵M. J. Frisch, G. W. Trucks, H. B. Schlegel, G. E. Scuseria, M. A. Robb, J. R. Cheeseman, G. Scalmani, V. Barone, G. A. Petersson, H. Nakatsuji, X. Li, M. Caricato, A. V. Marenich, J. Bloino, B. G. Janesko, R. Gomperts, B. Mennucci, H. P. Hratchian, J. V. Ortiz, A. F. Izmaylov, J. L. Sonnenberg, D. Williams-Young, F. Ding, F. Lipparini, F. Egidi, J. Goings, B. Peng, A. Petrone, T. Henderson, D. Ranasinghe, V. G. Zakrzewski, J. Gao, N. Rega, G. Zheng, W. Liang, M. Hada, M. Ehara, K. Toyota, R. Fukuda, J. Hasegawa, M. Ishida, T. Nakajima, Y. Honda, O. Kitao, H. Nakai, T. Vreven, K. Throssell, J. A. Montgomery, J. E. Peralta, Jr., F. Ogliaro, M. J. Bearpark, J. J. Heyd, E. N. Brothers, K. N. Kudin, V. N. Staroverov, T. A. Keith, R. Kobayashi, J. Normand, K. Raghavachari, A. P. Rendell, J. C. Burant, S. S. Iyengar, J. Tomasi, M. Cossi, J. M. Millam, M. Klene, C. Adamo, R. Cammi, J. W. Ochterski, R. L. Martin, K. Morokuma, O. Farkas, J. B. Foresman, and D. J. Fox, *GAUSSIAN 16*, Revision I.11, Gaussian, Inc., Wallingford, CT, 2016, development version.
- ⁴⁶R. Dennington, T. A. Keith, and J. M. Millam, *Gaussview version 6*, Semichem, Inc., Shawnee Mission KS, 2016.
- ⁴⁷G. Schaftenaar and J. H. N. Molden, "A pre- and post-processing program for molecular and electronic structures," *J. Comput.-Aided Mol. Des.* **14**, 123–134 (2000).